Evidence for the Rare Decay $B \to K^* \ell^+ \ell^-$ and Measurement of the $B \to K \ell^+ \ell^-$ Branching Fraction

B. Aubert,[1] R. Barate,[1] D. Boutigny,[1] J.-M. Gaillard,[1] A. Hicheur,[1] Y. Karyotakis,[1] J. P. Lees,[1] P. Robbe,[1] V. Tisserand,[1] A. Zghiche,[1] A. Palano,[2] A. Pompili,[2] J. C. Chen,[3] N. D. Qi,[3] G. Rong,[3] P. Wang,[3] Y. S. Zhu,[3] G. Eigen,[4] I. Ofte,[4] B. Stugu,[4] G. S. Abrams,[5] A.W. Borgland,[5] A. B. Breon,[5] D. N. Brown,[5] J. Button-Shafer,[5] R. N. Cahn,[5] E. Charles,[5] C. T. Day,[5] M. S. Gill,[5] A.V. Gritsan,[5] Y. Groysman,[5] R. G. Jacobsen,[5] R.W. Kadel,[5] J. Kadyk,[5] L. T. Kerth,[5] Yu. G. Kolomensky,[5] J. F. Kral,[5] G. Kukartsev,[5] C. LeClerc,[5] M. E. Levi,[5] G. Lynch,[5] L. M. Mir,[5] P. J. Oddone,[5] T. J. Orimoto,[5] M. Pripstein,[5] N. A. Roe,[5] A. Romosan,[5] M. T. Ronan,[5] V. G. Shelkov,[5] A.V. Telnov,[5] W. A. Wenzel,[5] K. Ford,[6] T. J. Harrison,[6] C. M. Hawkes,[6] D. J. Knowles,[6] S. E. Morgan,[6] R. C. Penny,[6] A. T. Watson,[6] N. K. Watson,[6] K. Goetzen,[7] T. Held,[7] H. Koch,[7] B. Lewandowski,[7] M. Pelizaeus,[7] K. Peters,[7] H. Schmuecker,[7] M. Steinke,[7] N. R. Barlow,[8] J. T. Boyd,[8] N. Chevalier,[8] W. N. Cottingham,[8] M. P. Kelly,[8] T. E. Latham,[8] C. Mackay,[8] F. F. Wilson,[8] K. Abe,[9] T. Cuhadar-Donszelmann,[9] C. Hearty,[9] T. S. Mattison,[9] J. A. McKenna,[9] D. Thiessen,[9] P. Kyberd,[10] A. K. McKemey,[10] V. E. Blinov,[11] A. D. Bukin,[11] V. B. Golubev,[11] V. N. Ivanchenko,[11] E. A. Kravchenko,[11] A. P. Onuchin,[11] S. I. Serednyakov,[11] Yu. I. Skovpen,[11] E. P. Solodov,[11] A. N. Yushkov,[11] D. Best,[12] M. Bruinsma,[12] M. Chao,[12] D. Kirkby,[12] A. J. Lankford,[12] M. Mandelkern,[12] R. K. Mommsen,[12] W. Roethel,[12] D. P. Stoker,[12] C. Buchanan,[13] B. L. Hartfiel,[13] B. C. Shen,[14] D. del Re,[15] H. K. Hadavand,[15] E. J. Hill,[15] D. B. MacFarlane,[15] H. P. Paar,[15] Sh. Rahatlou,[15] V. Sharma,[15] J.W. Berryhill,[16] C. Campagnari,[16] B. Dahmes,[16] N. Kuznetsova,[16] S. L. Levy,[16] O. Long,[16] A. Lu,[16] M. A. Mazur,[16] J. D. Richman,[16] W. Verkerke,[16] T.W. Beck,[17] J. Beringer,[17] A. M. Eisner,[17] C. A. Heusch,[17] W. S. Lockman,[17] T. Schalk,[17] R. E. Schmitz,[17] B. A. Schumm,[17] A. Seiden,[17] M. Turri,[17] W. Walkowiak,[17] D. C. Williams,[17] M. G. Wilson,[17] J. Albert,[18] E. Chen,[18] G. P. Dubois-Felsmann,[18] A. Dvoretskii,[18] D. G. Hitlin,[18] I. Narsky,[18] F. C. Porter,[18] A. Ryd,[18] A. Samuel,[18] S. Yang,[18] S. Jayatilleke,[19] G. Mancinelli,[19] B. T. Meadows,[19] M. D. Sokoloff,[19] T. Abe,[20] F. Blanc,[20] P. Bloom,[20] S. Chen,[20] P. J. Clark,[20] W. T. Ford,[20] U. Nauenberg,[20] A. Olivas,[20] P. Rankin,[20] J. Roy,[20] J. G. Smith,[20] W. C. van Hoek,[20] L. Zhang,[20] J. L. Harton,[21] T. Hu,[21] A. Soffer,[21] W. H. Toki,[21] R. J. Wilson,[21] J. Zhang,[21] D. Altenburg,[22] T. Brandt,[22] J. Brose,[22] T. Colberg,[22] M. Dickopp,[22] R. S. Dubitzky,[22] A. Hauke,[22] H. M. Lacker,[22] E. Maly,[22] R. Müller-Pfefferkorn,[22] R. Nogowski,[22] S. Otto,[22] J. Schubert,[22] K. R. Schubert,[22] R. Schwierz,[22] B. Spaan,[22] L. Wilden,[22] D. Bernard,[23] G. R. Bonneaud,[23] F. Brochard,[23] J. Cohen-Tanugi,[23] P. Grenier,[23] Ch. Thiebaux,[23] G. Vasileiadis,[23] M. Verderi,[23] A. Khan,[24] D. Lavin,[24] F. Muheim,[24] S. Playfer,[24] J. E. Swain,[24] M. Andreotti,[25] V. Azzolini,[25] D. Bettoni,[25] C. Bozzi,[25] R. Calabrese,[25] G. Cibinetto,[25] E. Luppi,[25] M. Negrini,[25] L. Piemontese,[25] A. Sarti,[25] E. Treadwell,[26] F. Anulli,[27,*] R. Baldini-Ferroli,[27] M. Biasini,[27,*] A. Calcaterra,[27] R. de Sangro,[27] D. Falciai,[27] G. Finocchiaro,[27] P. Patteri,[27] I. M. Peruzzi,[27,*] M. Piccolo,[27] M. Pioppi,[27,*] A. Zallo,[27] A. Buzzo,[28] R. Capra,[28] R. Contri,[28] G. Crosetti,[28] M. Lo Vetere,[28] M. Macri,[28] M. R. Monge,[28] S. Passaggio,[28] C. Patrignani,[28] E. Robutti,[28] A. Santroni,[28] S. Tosi,[28] S. Bailey,[29] M. Morii,[29] E. Won,[29] W. Bhimji,[30] D. A. Bowerman,[30] P. D. Dauncey,[30] U. Egede,[30] I. Eschrich,[30] J. R. Gaillard,[30] G.W. Morton,[30] J. A. Nash,[30] P. Sanders,[30] G. P. Taylor,[30] G. J. Grenier,[31] S.-J. Lee,[31] U. Mallik,[31] J. Cochran,[32] H. B. Crawley,[32] J. Lamsa,[32] W. T. Meyer,[32] S. Prell,[32] E. I. Rosenberg,[32] J. Yi,[32] M. Davier,[33] G. Grosdidier,[33] A. Höcker,[33] S. Laplace,[33] F. Le Diberder,[33] V. Lepeltier,[33] A. M. Lutz,[33] T. C. Petersen,[33] S. Plaszczynski,[33] M. H. Schune,[33] L. Tantot,[33] G. Wormser,[33] V. Brigljević,[34] C. H. Cheng,[34] D. J. Lange,[34] D. M. Wright,[34] A. J. Bevan,[35] J. P. Coleman,[35] J. R. Fry,[35] E. Gabathuler,[35] R. Gamet,[35] M. Kay,[35] R. J. Parry,[35] D. J. Payne,[35] R. J. Sloane,[35] C. Touramanis,[35] J. J. Back,[36] P. F. Harrison,[36] H.W. Shorthouse,[36] P. Strother,[36] P. B. Vidal,[36] C. L. Brown,[37] G. Cowan,[37] R. L. Flack,[37] H. U. Flaecher,[37] S. George,[37] M. G. Green,[37] A. Kurup,[37] C. E. Marker,[37] T. R. McMahon,[37] S. Ricciardi,[37] F. Salvatore,[37] G. Vaitsas,[37] M. A. Winter,[37] D. Brown,[38] C. L. Davis,[38] J. Allison,[39] R. J. Barlow,[39] A. C. Forti,[39] P. A. Hart,[39] M. C. Hodgkinson,[39] F. Jackson,[39] G. D. Lafferty,[39] A. J. Lyon,[39] J. H. Weatherall,[39] J. C. Williams,[39] A. Farbin,[40] A. Jawahery,[40] D. Kovalskyi,[40] C. K. Lae,[40] V. Lillard,[40] D. A. Roberts,[40] G. Blaylock,[41] C. Dallapiccola,[41] K. T. Flood,[41] S. S. Hertzbach,[41] R. Kofler,[41] V. B. Koptchev,[41] T. B. Moore,[41] S. Saremi,[41] H. Staengle,[41] S. Willocq,[41] R. Cowan,[42] G. Sciolla,[42] F. Taylor,[42] R. K. Yamamoto,[42] D. J. J. Mangeol,[43] P. M. Patel,[43] A. Lazzaro,[44] F. Palombo,[44] J. M. Bauer,[45] L. Cremaldi,[45] V. Eschenburg,[45] R. Godang,[45] R. Kroeger,[45] J. Reidy,[45] D. A. Sanders,[45] D. J. Summers,[45] H.W. Zhao,[45] S. Brunet,[46] D. Cote-Ahern,[46] C. Hast,[46] P. Taras,[46] H. Nicholson,[47] C. Cartaro,[48] N. Cavallo,[48,†] G. De Nardo,[48] F. Fabozzi,[48,†] C. Gatto,[48] L. Lista,[48] P. Paolucci,[48] D. Piccolo,[48] C. Sciacca,[48] M. A. Baak,[49] G. Raven,[49] J. M. LoSecco,[50] T. A. Gabriel,[51] B. Brau,[52] K. K. Gan,[52] K. Honscheid,[52] D. Hufnagel,[52] H. Kagan,[52] R. Kass,[52] T. Pulliam,[52] Q. K. Wong,[52] J. Brau,[53] R. Frey,[53] C. T. Potter,[53] N. B. Sinev,[53] D. Strom,[53] E. Torrence,[53] F. Colecchia,[54]

A. Dorigo,[54] F. Galeazzi,[54] M. Margoni,[54] M. Morandin,[54] M. Posocco,[54] M. Rotondo,[54] F. Simonetto,[54] R. Stroili,[54] G. Tiozzo,[54] C. Voci,[54] M. Benayoun,[55] H. Briand,[55] J. Chauveau,[55] P. David,[55] Ch. de la Vaissière,[55] L. Del Buono,[55] O. Hamon,[55] M. J. J. John,[55] Ph. Leruste,[55] J. Ocariz,[55] M. Pivk,[55] L. Roos,[55] J. Stark,[55] S. T'Jampens,[55] G. Therin,[55] P. F. Manfredi,[56] V. Re,[56] P. K. Behera,[57] L. Gladney,[57] Q. H. Guo,[57] J. Panetta,[57] C. Angelini,[58] G. Batignani,[58] S. Bettarini,[58] M. Bondioli,[58] F. Bucci,[58] G. Calderini,[58] M. Carpinelli,[58] V. Del Gamba,[58] F. Forti,[58] M. A. Giorgi,[58] A. Lusiani,[58] G. Marchiori,[58] F. Martinez-Vidal,[58,‡] M. Morganti,[58] N. Neri,[58] E. Paoloni,[58] M. Rama,[58] G. Rizzo,[58] F. Sandrelli,[58] J. Walsh,[58] M. Haire,[59] D. Judd,[59] K. Paick,[59] D. E. Wagoner,[59] N. Danielson,[60] P. Elmer,[60] C. Lu,[60] V. Miftakov,[60] J. Olsen,[60] A. J. S. Smith,[60] H. A. Tanaka,[60] E. W. Varnes,[60] F. Bellini,[61] G. Cavoto,[60,61] R. Faccini,[15,61] F. Ferrarotto,[61] F. Ferroni,[61] M. Gaspero,[61] M. A. Mazzoni,[61] S. Morganti,[61] M. Pierini,[61] G. Piredda,[61] F. Safai Tehrani,[61] C. Voena,[61] S. Christ,[62] G. Wagner,[62] R. Waldi,[62] T. Adye,[63] N. De Groot,[63] B. Franek,[63] N. I. Geddes,[63] G. P. Gopal,[63] E. O. Olaiya,[63] S. M. Xella,[63] R. Aleksan,[64] S. Emery,[64] A. Gaidot,[64] S. F. Ganzhur,[64] P.-F. Giraud,[64] G. Hamel de Monchenault,[64] W. Kozanecki,[64] M. Langer,[64] M. Legendre,[64] G. W. London,[64] B. Mayer,[64] G. Schott,[64] G. Vasseur,[64] Ch. Yeche,[64] M. Zito,[64] M. V. Purohit,[65] A. W. Weidemann,[65] F. X. Yumiceva,[65] D. Aston,[66] R. Bartoldus,[66] N. Berger,[66] A. M. Boyarski,[66] O. L. Buchmueller,[66] M. R. Convery,[66] D. P. Coupal,[66] D. Dong,[66] J. Dorfan,[66] D. Dujmic,[66] W. Dunwoodie,[66] R. C. Field,[66] T. Glanzman,[66] S. J. Gowdy,[66] E. Grauges-Pous,[66] T. Hadig,[66] V. Halyo,[66] T. Hryn'ova,[66] W. R. Innes,[66] C. P. Jessop,[66] M. H. Kelsey,[66] P. Kim,[66] M. L. Kocian,[66] U. Langenegger,[66] D. W. G. S. Leith,[66] S. Luitz,[66] V. Luth,[66] H. L. Lynch,[66] H. Marsiske,[66] R. Messner,[66] D. R. Muller,[66] C. P. O'Grady,[66] V. E. Ozcan,[66] A. Perazzo,[66] M. Perl,[66] S. Petrak,[66] B. N. Ratcliff,[66] S. H. Robertson,[66] A. Roodman,[66] A. A. Salnikov,[66] R. H. Schindler,[66] J. Schwiening,[66] G. Simi,[66] A. Snyder,[66] A. Soha,[66] J. Stelzer,[66] D. Su,[66] M. K. Sullivan,[66] J. Va'vra,[66] S. R. Wagner,[66] M. Weaver,[66] A. J. R. Weinstein,[66] W. J. Wisniewski,[66] D. H. Wright,[66] C. C. Young,[66] P. R. Burchat,[67] A. J. Edwards,[67] T. I. Meyer,[67] B. A. Petersen,[67] C. Roat,[67] S. Ahmed,[68] M. S. Alam,[68] J. A. Ernst,[68] M. Saleem,[68] F. R. Wappler,[68] W. Bugg,[69] M. Krishnamurthy,[69] S. M. Spanier,[69] R. Eckmann,[70] H. Kim,[70] J. L. Ritchie,[70] R. F. Schwitters,[70] J. M. Izen,[71] I. Kitayama,[71] X. C. Lou,[71] S. Ye,[71] F. Bianchi,[72] M. Bona,[72] F. Gallo,[72] D. Gamba,[72] C. Borean,[73] L. Bosisio,[73] G. Della Ricca,[73] S. Dittongo,[73] S. Grancagnolo,[73] L. Lanceri,[73] P. Poropat,[73,§] L. Vitale,[73] G. Vuagnin,[73] R. S. Panvini,[74] Sw. Banerjee,[75] C. M. Brown,[75] D. Fortin,[75] P. D. Jackson,[75] R. Kowalewski,[75] J. M. Roney,[75] H. R. Band,[76] S. Dasu,[76] M. Datta,[76] A. M. Eichenbaum,[76] J. R. Johnson,[76] P. E. Kutter,[76] H. Li,[76] R. Liu,[76] F. Di Lodovico,[76] A. Mihalyi,[76] A. K. Mohapatra,[76] Y. Pan,[76] R. Prepost,[76] S. J. Sekula,[76] J. H. von Wimmersperg-Toeller,[76] J. Wu,[76] S. L. Wu,[76] Z. Yu,[76] and H. Neal[77]

(*BABAR* Collaboration)

[1]*Laboratoire de Physique des Particules, F-74941 Annecy-le-Vieux, France*
[2]*Università di Bari, Dipartimento di Fisica and INFN, I-70126 Bari, Italy*
[3]*Institute of High Energy Physics, Beijing 100039, China*
[4]*University of Bergen, Institute of Physics, N-5007 Bergen, Norway*
[5]*Lawrence Berkeley National Laboratory and University of California, Berkeley, California 94720, USA*
[6]*University of Birmingham, Birmingham B15 2TT, United Kingdom*
[7]*Ruhr Universität Bochum, Institut für Experimentalphysik 1, D-44780 Bochum, Germany*
[8]*University of Bristol, Bristol BS8 1TL, United Kingdom*
[9]*University of British Columbia, Vancouver, British Columbia, Canada V6T 1Z1*
[10]*Brunel University, Uxbridge, Middlesex UB8 3PH, United Kingdom*
[11]*Budker Institute of Nuclear Physics, Novosibirsk 630090, Russia*
[12]*University of California at Irvine, Irvine, California 92697, USA*
[13]*University of California at Los Angeles, Los Angeles, California 90024, USA*
[14]*University of California at Riverside, Riverside, California 92521, USA*
[15]*University of California at San Diego, La Jolla, California 92093, USA*
[16]*University of California at Santa Barbara, Santa Barbara, California 93106, USA*
[17]*University of California at Santa Cruz, Institute for Particle Physics, Santa Cruz, California 95064, USA*
[18]*California Institute of Technology, Pasadena, California 91125, USA*
[19]*University of Cincinnati, Cincinnati, Ohio 45221, USA*
[20]*University of Colorado, Boulder, Colorado 80309, USA*
[21]*Colorado State University, Fort Collins, Colorado 80523, USA*
[22]*Technische Universität Dresden, Institut für Kern- und Teilchenphysik, D-01062 Dresden, Germany*
[23]*Ecole Polytechnique, LLR, F-91128 Palaiseau, France*
[24]*University of Edinburgh, Edinburgh EH9 3JZ, United Kingdom*
[25]*Università di Ferrara, Dipartimento di Fisica and INFN, I-44100 Ferrara, Italy*
[26]*Florida A&M University, Tallahassee, Florida 32307, USA*

[27]Laboratori Nazionali di Frascati dell'INFN, I-00044 Frascati, Italy

[28]Università di Genova, Dipartimento di Fisica and INFN, I-16146 Genova, Italy

[29]Harvard University, Cambridge, Massachusetts 02138, USA

[30]Imperial College London, London SW7 2BW, United Kingdom

[31]University of Iowa, Iowa City, Iowa 52242, USA

[32]Iowa State University, Ames, Iowa 50011-3160, USA

[33]Laboratoire de l'Accélérateur Linéaire, F-91898 Orsay, France

[34]Lawrence Livermore National Laboratory, Livermore, California 94550, USA

[35]University of Liverpool, Liverpool L69 3BX, United Kingdom

[36]Queen Mary, University of London, E1 4NS, United Kingdom

[37]University of London, Royal Holloway and Bedford New College, Egham, Surrey TW20 0EX, United Kingdom

[38]University of Louisville, Louisville, Kentucky 40292, USA

[39]University of Manchester, Manchester M13 9PL, United Kingdom

[40]University of Maryland, College Park, Maryland 20742, USA

[41]University of Massachusetts, Amherst, Massachusetts 01003, USA

[42]Massachusetts Institute of Technology, Laboratory for Nuclear Science, Cambridge, Massachusetts 02139, USA

[43]McGill University, Montréal, Quebec, Canada H3A 2T8

[44]Università di Milano, Dipartimento di Fisica and INFN, I-20133 Milano, Italy

[45]University of Mississippi, University, Mississippi 38677, USA

[46]Université de Montréal, Laboratoire René J. A. Lévesque, Montréal, Quebec, Canada H3C 3J7

[47]Mount Holyoke College, South Hadley, Massachusetts 01075

[48]Università di Napoli Federico II, Dipartimento di Scienze Fisiche and INFN, I-80126, Napoli, Italy

[49]NIKHEF, National Institute for Nuclear Physics and High Energy Physics, NL-1009 DB Amsterdam, The Netherlands

[50]University of Notre Dame, Notre Dame, Indiana 46556, USA

[51]Oak Ridge National Laboratory, Oak Ridge, Tennessee 37831, USA

[52]The Ohio State University, Columbus, Ohio 43210, USA

[53]University of Oregon, Eugene, Oregon 97403, USA

[54]Università di Padova, Dipartimento di Fisica and INFN, I-35131 Padova, Italy

[55]Universités Paris VI et VII, Lab de Physique Nucléaire H. E., F-75252 Paris, France

[56]Università di Pavia, Dipartimento di Elettronica and INFN, I-27100 Pavia, Italy

[57]University of Pennsylvania, Philadelphia, Pennsylvania 19104, USA

[58]Università di Pisa, Dipartimento di Fisica, Scuola Normale Superiore and INFN, I-56127 Pisa, Italy

[59]Prairie View A&M University, Prairie View, Texas 77446, USA

[60]Princeton University, Princeton, New Jersey 08544, USA

[61]Università di Roma La Sapienza, Dipartimento di Fisica and INFN, I-00185 Roma, Italy

[62]Universität Rostock, D-18051 Rostock, Germany

[63]Rutherford Appleton Laboratory, Chilton, Didcot, Oxon OX11 0QX, United Kingdom

[64]DSM/Dapnia, CEA/Saclay, F-91191 Gif-sur-Yvette, France

[65]University of South Carolina, Columbia, South Carolina 29208, USA

[66]Stanford Linear Accelerator Center, Stanford, California 94309, USA

[67]Stanford University, Stanford, California 94305-4060, USA

[68]State University of New York, Albany, New York 12222, USA

[69]University of Tennessee, Knoxville, Tennessee 37996, USA

[70]University of Texas at Austin, Austin, Texas 78712, USA

[71]University of Texas at Dallas, Richardson, Texas 75083, USA

[72]Università di Torino, Dipartimento di Fisica Sperimentale and INFN, I-10125 Torino, Italy

[73]Università di Trieste, Dipartimento di Fisica and INFN, I-34127 Trieste, Italy

[74]Vanderbilt University, Nashville, Tennessee 37235, USA

[75]University of Victoria, Victoria, British Columbia, Canada V8W 3P6

[76]University of Wisconsin, Madison, Wisconsin 53706, USA

[77]Yale University, New Haven, Connecticut 06511, USA

We present evidence for the flavor-changing neutral current decay $B \to K^* \ell^+ \ell^-$ and a measurement of the branching fraction for the related process $B \to K \ell^+ \ell^-$, where $\ell^+ \ell^-$ is either an $e^+ e^-$ or a $\mu^+ \mu^-$ pair. These decays are highly suppressed in the standard model, and they are sensitive to contributions from new particles in the intermediate state. The data sample comprises 123×10^6 $\Upsilon(4S) \to B\overline{B}$ decays collected with the *BABAR* detector at the SLAC PEP-II $e^+ e^-$ storage ring. Averaging over $K^{(*)}$ isospin and lepton flavor, we obtain the branching fractions $\mathcal{B}(B \to K \ell^+ \ell^-) = (0.65^{+0.14}_{-0.13} \pm 0.04) \times 10^{-6}$ and $\mathcal{B}(B \to K^* \ell^+ \ell^-) = (0.88^{+0.33}_{-0.29} \pm 0.10) \times 10^{-6}$, where the uncertainties are statistical and systematic, respectively. The significance of the $B \to K \ell^+ \ell^-$ signal is over 8σ, while for $B \to K^* \ell^+ \ell^-$ it is 3.3σ.

Rare decays of B mesons that involve loop diagrams in the standard model (SM) provide a promising means to search for effects beyond the SM [1]. The decays $B \to K\ell^+\ell^-$ and $B \to K^*\ell^+\ell^-$, where $\ell^{\pm}$ are charged leptons and K^* is the $K^*(892)$ meson, result from one-loop processes that transform the b quark in the initial-state B meson into an s quark in the final-state $K^{(*)}$ meson. In the SM, three amplitudes contribute at leading order: an electromagnetic (EM) penguin, a Z penguin, and a W^+W^- box diagram. The penguin diagrams involve the emission and absorption of a W boson. The presence of three SM electroweak amplitudes makes $B \to K^{(*)}\ell^+\ell^-$ more complex than $B \to K^*\gamma$, which proceeds solely through an EM penguin.

Because of their loop structure, these decays are highly suppressed, with SM branching fractions expected to be roughly 0.5×10^{-6} for $B \to K\ell^+\ell^-$ and about 3 times that for the $B \to K^*\ell^+\ell^-$ modes [1–3]. Because of the complexity of strong interaction effects, however, theoretical uncertainties on the rates are currently at least 35% (Ali *et al.* [1]). Both $B \to K^*e^+e^-$ and $B \to K^*\mu^+\mu^-$ receive a contribution from the pole in the EM penguin amplitude at $q^2 = m_{\ell^+\ell^-}^2 = 0$, but the enhancement in the electron mode is significantly larger due to a lower q^2 threshold. This pole does not contribute to $B \to Ke^+e^-$ or to $B \to K\mu^+\mu^-$; thus, the difference in those partial widths is expected to be negligible. An important consequence of the loop structure of these decays is that their branching fractions and kinematic distributions can be significantly affected by the presence of new particles or couplings, such as those predicted in models based on supersymmetry [1].

Recently, substantial progress has been made in experimental studies of these decays. The Belle Collaboration has observed $B \to K\ell^+\ell^-$, as well as the inclusive $B \to X_s\ell^+\ell^-$ decay [4]. Limits on these and similar modes have been set by *BABAR* [5], Belle [4], CLEO [6], and CDF [7]. Our new measurements are based on a data sample 6 times larger than that used for our previously published results. We study eight final states: $B^+ \to K^+\ell^+\ell^-$, $B^0 \to K_S^0\ell^+\ell^-$, $B^+ \to K^{*+}\ell^+\ell^-$, and $B^0 \to K^{*0}\ell^+\ell^-$, where $K^{*0} \to K^+\pi^-$, $K^{*+} \to K_S^0\pi^+$, $K_S^0 \to \pi^+\pi^-$, and ℓ is either an e or a μ. Throughout this Letter, charge-conjugate modes are implied.

We analyze data collected with the *BABAR* detector [8] at the PEP-II storage ring at the Stanford Linear Accelerator Center. The data sample comprises 113.1 fb^{-1} recorded on the $\Upsilon(4S)$ resonance, yielding $(122.9 \pm 1.4) \times 10^6$ $B\overline{B}$ decays, and an off-resonance sample of 12.0 fb^{-1} used to study continuum background.

We select events that include two oppositely charged leptons (e^+e^-, $\mu^+\mu^-$), a kaon (either $K^{\pm}$ or K_S^0), and, for the $B \to K^*\ell^+\ell^-$ modes, a $\pi^{\pm}$ that combines with a kaon to form a K^* candidate. Electrons are identified primarily in the CsI(Tl) electromagnetic calorimeter, while muons are identified by their penetration through iron plates of the magnet flux return. Electron (muon) candidates are

required to satisfy $p > 0.5$ (1.0) GeV/c. Bremsstrahlung photons from electrons are recovered by combining an electron candidate with up to one photon with $E > 30$ MeV in a small angular region around the initial electron direction. Photon conversions and π^0 Dalitz decays are removed by vetoing all low-mass e^+e^- pairs, except in $B \to K^*e^+e^-$ modes, where we preserve acceptance at low mass by retaining pairs that intersect inside the beam pipe.

$K^{\pm}$ candidates are tracks with dE/dx and Cherenkov angle consistent with a kaon. $\pi^{\pm}$ candidates are tracks that do not satisfy the $K^{\pm}$ selection. K_S^0 candidates are reconstructed from two oppositely charged tracks with an invariant mass consistent with the K_S^0 mass and a common vertex displaced from the primary vertex by at least 1 mm.

True B signal decays produce narrow peaks in the distributions of two kinematic variables, which can be fitted to extract the signal and background yields. For a candidate system of B daughter particles with masses m_i and three-momenta $\mathbf{p}_i^*$ in the $\Upsilon(4S)$ center-of-mass (CM) frame, we define $m_{\mathrm{ES}} = \sqrt{E_b^{*2} - |\sum_i \mathbf{p}_i^*|^2}$ and $\Delta E = \sum_i \sqrt{m_i^2 + \mathbf{p}_i^{*2}} - E_b^*$, where E_b^* is the beam energy in the CM frame. For signal events, the m_{ES} distribution peaks at the B meson mass with resolution $\sigma \approx 2.5$ MeV/c^2, and the ΔE distribution peaks near zero, with a typical width $\sigma \approx 20$ MeV. In $B \to K\ell^+\ell^-$ channels, we perform a two-dimensional unbinned maximum-likelihood fit to the distribution of m_{ES} and ΔE in the region $m_{\mathrm{ES}} > 5.2$ GeV/c^2 and $|\Delta E| < 0.25$ GeV. In $B \to K^*\ell^+\ell^-$ decays, we perform a three-dimensional fit to m_{ES}, ΔE, and the kaon-pion invariant mass in the region $0.7 < m_{K\pi} < 1.1$ GeV/c^2.

Backgrounds arise from three main sources: random combinations of particles from $q\bar{q}$ events produced in the continuum, random combinations of particles from $\Upsilon(4S) \to B\overline{B}$ decays, and B decays to topologies similar to the signal modes. The first two ("combinatorial") backgrounds typically arise from pairs of semileptonic decays and produce broad distributions in m_{ES} and ΔE compared to the signal. The third source arises from modes such as $B \to J/\psi K^{(*)}$ (with $J/\psi \to \ell^+\ell^-$) or $B \to K^{(*)}\pi\pi$ (with pions misidentified as muons), which have shapes similar to the signal. All selection criteria are optimized with GEANT4 [9] simulated data or with data samples outside the full fit region.

We suppress combinatorial background from continuum processes using a Fisher discriminant [10], which is a linear combination of variables with coefficients optimized to distinguish between signal and background. The variables (defined in the CM frame) are (1) the ratio of second- to zeroth-order Fox-Wolfram moments [11] for the event, computed using all charged tracks and neutral energy clusters; (2) the angle between the thrust axis of the B candidate and that of the remaining particles in the event; (3) the production angle θ_B of the B candidate with

respect to the beam axis; and (4) the masses of $K\ell$ pairs with charge correlation consistent with D decay.

We suppress combinatorial backgrounds from $B\overline{B}$ events using a likelihood function constructed from (1) the missing energy of the event, computed from all charged tracks and neutral energy clusters, (2) the vertex fit probability of all tracks from the B candidate, (3) the vertex fit probability of the two leptons, and (4) the angle θ_B. Missing energy provides the strongest suppression of combinatorial $B\overline{B}$ background events, which typically contain neutrinos from two semileptonic decays.

The most prominent backgrounds that peak in m_{ES} and ΔE are B decays to charmonium: $B \to J/\psi K^{(*)}$ (with $J/\psi \to \ell^+\ell^-$) and analogous B decays to $\psi(2S)$. We exclude dilepton pairs consistent with the J/ψ ($2.90 < m_{e^+e^-} < 3.20$ GeV/c^2 and $3.00 < m_{\mu^+\mu^-} < 3.20$ GeV/c^2) or with the $\psi(2S)$ ($3.60 < m_{\ell^+\ell^-} < 3.75$ GeV/c^2). This veto is also applied to $m_{e^+e^-}$ computed without bremsstrahlung photon recovery. When a lepton radiates or is mismeasured, $m_{\ell^+\ell^-}$ can shift away from the charmonium mass, while ΔE shifts in a correlated manner. The veto region is extended in the ($m_{\ell^+\ell^-}$, ΔE) plane to account for this correlation, removing nearly all charmonium events and simplifying the description of the background in the fit. Because the charmonium events removed by these vetoes are so similar to signal events, these modes provide extensive control samples (about 5200 events in all) for studying signal shapes, selection efficiencies, and systematic errors. Outside the charmonium veto regions, the signal efficiency is similar over the full q^2 range of each mode.

In muon modes, where the probability for a hadron to be misidentified as a muon can be as high as a few percent, background from the decay $B^- \to D^0\pi^-$ with $D^0 \to K^-\pi^+$ or $D^0 \to K^{*-}\pi^+$, or from $\overline{B}^0 \to D^+\pi^-$ with $D^+ \to \overline{K}^{*0}\pi^+$, is significant. These events are suppressed by vetoing events where the $K^{(*)}\mu$ kinematics are consistent with those of a hadronic D decay.

We estimate the residual peaking background from measurements in the data, supplemented in some cases by simulation studies. Events from $B \to K^{(*)}\pi\pi$, $B \to K^{(*)}K\pi$, and $B \to K^{(*)}KK$ are highly suppressed by the particle identification criteria. These backgrounds are estimated from control samples to be 0.19 ± 0.11 events per channel averaged over muon modes and less than 0.01 events per channel in electron modes. After the vetoes on $B \to J/\psi K^{(*)}$ and $B \to \psi(2S)K^{(*)}$ decays, the remaining peaking background is estimated from simulation to be 0.17 ± 0.07 events per channel averaged over $B \to K^*\ell^+\ell^-$ modes, and it is negligible in $B \to K\ell^+\ell^-$ modes. The background from $B \to K^*\gamma$ (with photon conversion in the detector) is determined from simulation to be 0.48 ± 0.16 events in $B^0 \to K^{*0}e^+e^-$ and 0.09 ± 0.04 events in $B^+ \to K^{*+}e^+e^-$.

The signal shapes are parametrized with a Gaussian core for m_{ES} and a double Gaussian core for ΔE. Both the m_{ES} and ΔE shapes include a radiative tail, which ac-

counts for the effects of bremsstrahlung. The m_{ES} shape parameters are assumed to have ΔE dependence $c_0 + c_2(\Delta E)^2$. All signal shape parameters are fixed from signal simulation, except for the mean and width parameters in m_{ES} (c_0 only) and ΔE, which are fixed to values from charmonium data control samples.

The background is modeled as the sum of three terms: (1) a combinatorial background shape with floating normalization, written as the product of an ARGUS function [12] in m_{ES}, an exponential in ΔE, and the product of $\sqrt{m_{K\pi} - m_K - m_\pi}$ and a quadratic function of $m_{K\pi}$ for the K^* modes; (2) a peaking background contribution, with the same shape as the signal, but with normalization fixed to measured peaking backgrounds; and (3) terms with floating normalization to describe (a) background in $B \to K\ell^+\ell^-$ ($B \to K^*\ell^+\ell^-$) from $B \to K^*\ell^+\ell^-$ ($B \to K^*\pi\ell^+\ell^-$) events with a lost pion, and (b) background in $B \to K^*\ell^+\ell^-$ from $B \to K\ell^+\ell^-$ events with a randomly added pion. In the K^* modes, we allow an additional background (4) that uses our combinatorial shape in m_{ES} and ΔE, but peaks in $m_{K\pi}$ at the K^* mass. Because the normalizations for terms (1), (3), and (4) are floating, as are the combinatorial background shape parameters, much of the uncertainty in the background is propagated into the statistical uncertainty on the signal yield obtained from the fit.

Table I lists signal yields and branching fractions for each mode. The relative systematic uncertainties on the efficiency, $\Delta\mathcal{B}_\epsilon/\mathcal{B}$, arise from charged-particle tracking (1.0% per lepton, 1.7% per charged hadron), particle identification (1.1% per electron, 1.6% per muon, 0.9% per pion, 0.9% per kaon), the continuum suppression cut [(0.8–2.8)%], the $B\overline{B}$ suppression cut [(1.4–5.0)%], K_S^0 selection (3.8%), signal simulation statistics [(0.7–1.4)%], theoretical model dependence of the efficiency [(4–7)%, depending on the mode], and the number of $B\overline{B}$ events (1.1%). Uncertainties on efficiencies due to model dependence of form factors are taken to be the full range of variation from a set of models [2].

The systematic uncertainties on the fit yields, $\Delta\mathcal{B}_{fit}$, arise from three sources: uncertainties in the parameters describing the signal shapes, possible correlation between m_{ES} and ΔE in the combinatorial background shape, and uncertainties in the peaking backgrounds. The uncertainties in the means and widths of the signal shapes are obtained by comparing data and simulation for the charmonium control samples. For modes with electrons, we also vary the fraction of signal events in the tail of the ΔE distribution. To evaluate sensitivity to the background parametrization, we allow additional parameters and a correlation between m_{ES} and ΔE.

Table I also lists results from simultaneous fits to combinations of $B \to K\ell^+\ell^-$ modes and combinations of $B \to K^*\ell^+\ell^-$ modes, where the relative branching fractions for the contributing modes are constrained. B^0 and B^+ production rates are constrained to be equal, and the ratio of their total widths is constrained to be

TABLE I. Results from the fits to $B \to K^{(*)}\ell^+\ell^-$ modes. The columns are, from left to right, fitted signal yield; the signal efficiency, ϵ (not including the branching fractions for K^* and K^0 decays); the fractional systematic error on the selection efficiency, $\Delta\mathcal{B}_\epsilon/\mathcal{B}$; the systematic error from the fit, $\Delta\mathcal{B}_{\text{fit}}$; and the branching fraction central value ($\mathcal{B}$) with its statistical and total systematic uncertainties. For the branching fractions averaged over different channels (lower part of table), simultaneous, constrained fits are performed to extract an efficiency-corrected signal yield that averages over the included channels. The modes with significance $>3\sigma$ are $K^+e^+e^-$ (8.4σ), $K^0\mu^+\mu^-$ (4.1σ), Ke^+e^- (7.8σ), $K\ell^+\ell^-$ (8.4σ), and $K^*\ell^+\ell^-$ (3.3σ).

Mode	Signal yield	ϵ (%)	$\Delta\mathcal{B}_\epsilon/\mathcal{B}$ (%)	$\Delta\mathcal{B}_{\text{fit}}$ (10^{-6})	$\mathcal{B}$ (10^{-6})
$K^+e^+e^-$	$24.7^{+5.9}_{-5.2}$	19.2	±6.3	±0.02	$1.05^{+0.25}_{-0.22}\pm0.07$
$K^+\mu^+\mu^-$	$0.7^{+2.0}_{-1.2}$	8.5	±7.6	±0.02	$0.07^{+0.19}_{-0.11}\pm0.02$
$K^0e^+e^-$	$-1.8^{+2.0}_{-1.4}$	20.1	±8.4	±0.08	$-0.21^{+0.23}_{-0.16}\pm0.08$
$K^0\mu^+\mu^-$	$5.9^{+3.0}_{-2.3}$	8.6	±8.8	±0.02	$1.63^{+0.82}_{-0.63}\pm0.14$
$K^{*0}e^+e^-$	$12.4^{+6.3}_{-5.2}$	13.6	±7.6	±0.08	$1.11^{+0.56}_{-0.47}\pm0.11$
$K^{*0}\mu^+\mu^-$	$4.5^{+4.1}_{-3.0}$	6.4	±10.1	±0.07	$0.86^{+0.79}_{-0.58}\pm0.11$
$K^{*+}e^+e^-$	$0.6^{+3.8}_{-2.5}$	10.2	±10.7	±0.28	$0.20^{+1.34}_{-0.87}\pm0.28$
$K^{*+}\mu^+\mu^-$	$4.2^{+3.5}_{-2.4}$	4.8	±12.7	±0.15	$3.07^{+2.58}_{-1.78}\pm0.42$
Ke^+e^-	91^{+22}_{-19}		±6.5	±0.02	$0.74^{+0.18}_{-0.16}\pm0.05$
$K\mu^+\mu^-$	55^{+29}_{-23}		±7.4	±0.01	$0.45^{+0.23}_{-0.19}\pm0.04$
$K\ell^+\ell^-$	80^{+17}_{-15}		±6.4	±0.01	$0.65^{+0.14}_{-0.13}\pm0.04$
$K^*e^+e^-$	121^{+61}_{-51}		±7.8	±0.08	$0.98^{+0.50}_{-0.42}\pm0.11$
$K^*\mu^+\mu^-$	156^{+94}_{-75}		±10.1	±0.09	$1.27^{+0.76}_{-0.61}\pm0.16$
$K^*\ell^+\ell^-$	108^{+41}_{-36}		±8.1	±0.07	$0.88^{+0.33}_{-0.29}\pm0.10$

1.085 ± 0.017 [13]. All branching fractions from simultaneous fits are expressed relative to the B^0 total width. The projections of the fit on m_{ES} and ΔE are shown in Fig. 1 for the simultaneous fit to the $B \to K\ell^+\ell^-$ channels. We assume that all four $B \to K\ell^+\ell^-$ modes have equal partial widths. A signal is evident at the B mass in
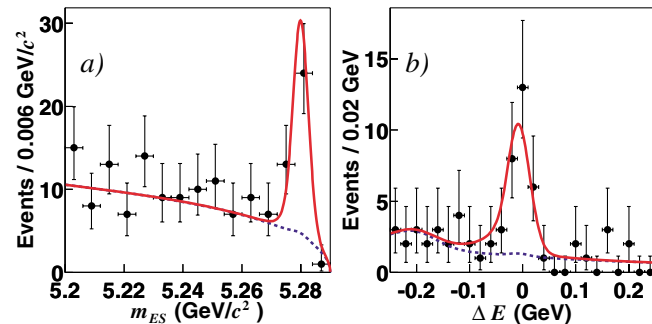

FIG. 1 (color online). Distributions of the fit variables in $K\ell^+\ell^-$ data (points), compared with projections of the simultaneous fit (curves): (a) m_{ES} distribution after requiring $-0.11 < \Delta E < 0.05$ GeV and (b) ΔE distribution after requiring $|m_{\text{ES}} - m_B| < 6.6$ MeV/c^2 (2.6σ). The solid curve is the sum of all fit components, including signal; the dashed curve is the sum of all background components.

m_{ES} and at $\Delta E = 0$. Figure 2 shows projections of the simultaneous fit to all $B \to K^*\ell^+\ell^-$ modes. Here, the partial width ratio of electron and muon modes is constrained to be $\Gamma(B \to K^*e^+e^-)/\Gamma(B \to K^*\mu^+\mu^-) = 1.33$ from the model of Ali et al. [1]. Our simultaneous fit result is expressed as a $B^0 \to K^{*0}\mu^+\mu^-$ branching fraction.

The significance of the $B \to K\ell^+\ell^-$ signal from the simultaneous fit is $\sim8\sigma$, computed as $\sqrt{2\Delta\log\mathcal{L}}$, where $\Delta\log\mathcal{L}$ is the likelihood difference between the best fit and the null-signal hypothesis. We account for systematic uncertainties in the significance by simultaneously including all effects that individually lower the fit yields prior to computing the change in likelihood. The significance of the $B \to K^*\ell^+\ell^-$ signal, including all systematic uncertainties, is 3.3σ (3.8σ not including them).

In summary, we have observed signals for $B \to K\ell^+\ell^-$, averaged over lepton type (e^+e^- and $\mu^+\mu^-$) and B charge, and we have obtained the first evidence for $B \to K^*\ell^+\ell^-$, similarly averaged. We obtain

$$\mathcal{B}(B \to K\ell^+\ell^-) = (0.65^{+0.14}_{-0.13} \pm 0.04) \times 10^{-6},$$
$$\mathcal{B}(B \to K^*\ell^+\ell^-) = (0.88^{+0.33}_{-0.29} \pm 0.10) \times 10^{-6},$$

where the first error is statistical and the second is systematic. Our branching fraction for $B \to K\ell^+\ell^-$ is slightly higher than our previous limit 0.51×10^{-6} (90% confidence level) [5] and is in agreement with the Belle result $(0.75^{+0.25}_{-0.21} \pm 0.09) \times 10^{-6}$ [4]. Our $B \to K^*\ell^+\ell^-$ branching fraction is consistent with previous 90% confidence level limits from BABAR ($<3.1 \times 10^{-6}$ for $K^*\ell^+\ell^-$) [5] and Belle ($<3.1 \times 10^{-6}$ for $K^*\mu^+\mu^-$) [4]. These results are consistent with the range of predictions based on the standard model [1–3].
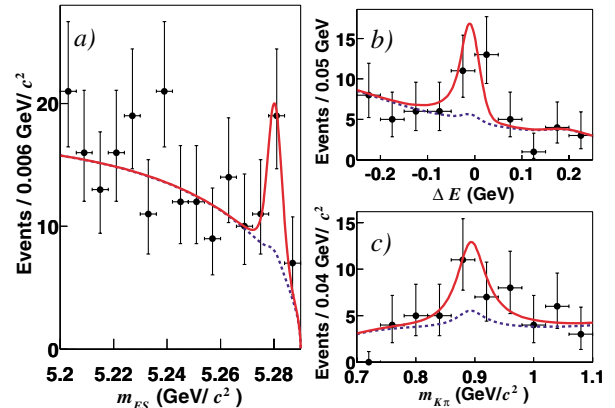

FIG. 2 (color online). Distributions of the fit variables in $K^*\ell^+\ell^-$ data (points), compared with projections of the simultaneous fit (curves): (a) m_{ES} after requiring $-0.11 < \Delta E < 0.05$ GeV and $0.817 < m_{K\pi} < 0.967$ GeV/c^2, (b) ΔE after requiring $|m_{\text{ES}} - m_B| < 6.6$ MeV/c^2 (2.6σ), $0.817 < m_{K\pi} < 0.967$ GeV/c^2, and (c) $m_{K\pi}$ after requiring $|m_{\text{ES}} - m_B| < 6.6$ MeV/c^2 and $-0.11 < \Delta E < 0.05$ GeV. The solid curve is the sum of all fit components, including signal; the dashed curve is the sum of all background components.

---

*Also with Università di Perugia, Perugia, Italy.

†Also with Università della Basilicata, Potenza, Italy.

‡Also with IFIC, Instituto de Física Corpuscular, CSIC-Universidad de Valencia, Valencia, Spain.

§Deceased.

[1] A. Ali *et al.*, Phys. Rev. D **66**, 034002 (2002); G. Burdman, Phys. Rev. D **52**, 6400 (1995); J. L. Hewett and J. D. Wells, Phys. Rev. D **55**, 5549 (1997).

[2] A. Ali *et al.*, Phys. Rev. D **61**, 074024 (2000); P. Colangelo *et al.*, Phys. Rev. D **53**, 3672 (1996); D. Melikhov, N. Nikitin, and S. Simula, Phys. Rev. D **57**, 6814 (1998).

[3] T. M. Aliev *et al.*, Phys. Lett. B **400**, 194 (1997); T. M. Aliev, M. Savci, and A. Özpineci, Phys. Rev. D **56**, 4260 (1997); C.-H. Chen and C. Q. Geng, Phys. Rev. D **66**, 094018 (2002); H.-M. Choi, C.-R. Ji, and L. S. Kisslinger, Phys. Rev. D **65**, 074032 (2002); N. G. Deshpande and J. Trampetic, Phys. Rev. Lett. **60**, 2583 (1988); A. Faessler *et al.*, EPJdirect C **4**, 18 (2002); C. Greub, A. Ioannissian, and D. Wyler, Phys. Lett. B **346**, 149 (1995); C. Q. Geng and C. P. Kao, Phys. Rev. D **54**, 5636 (1996); M. Zhong, Y. L. Wu, and W. Y. Wang, Int. J. Mod. Phys. A **18**, 1959 (2003).

[4] Belle Collaboration, K. Abe *et al.*, Phys. Rev. Lett. **88**, 021801 (2002); Belle Collaboration, J. Kaneko *et al.*, Phys. Rev. Lett. **90**, 021801 (2003).

[5] *BABAR* Collaboration, B. Aubert *et al.*, Phys. Rev. Lett. **88**, 241801 (2002).

[6] CLEO Collaboration, S. Anderson *et al.*, Phys. Rev. Lett. **87**, 181803 (2001).

[7] CDF Collaboration, T. Affolder *et al.*, Phys. Rev. Lett. **83**, 3378 (1999).

[8] *BABAR* Collaboration, B. Aubert *et al.*, Nucl. Instrum. Methods Phys. Res., Sect. A **479**, 1 (2001).

[9] S. Agostinelli *et al.*, Nucl. Instrum. Methods Phys. Res., Sect. A **506**, 250 (2003).

[10] R. A. Fisher, Ann. Eugenics **7**, 179 (1936).

[11] G. C. Fox and S. Wolfram, Phys. Rev. Lett. **41**, 1581 (1978).

[12] The function is $f(x) \propto x\sqrt{1-x^2}\exp[-\zeta(1-x^2)]$, where ζ is a fit parameter and $x = m_{ES}/E_b^*$; ARGUS Collaboration, H. Albrecht *et al.*, Z. Phys. C **48**, 543 (1990).

[13] Particle Data Group, K. Hagiwara *et al.*, Phys. Rev. D **66**, 010001 (2002).